Silver surface modifications under carbon dioxide hydrogenation conditions in the presence and absence of zinc oxide nanoparticles

Paul Maurice Leidinger[a†], Mirco Panighel[c ‡], Vitaly L. Sushkevich[a], Paolo Piseri[d, e], Alessandro Podestà[d], Jeroen A. van Bokhoven[a, b], Luca Artiglia[a]

[a.] *Center for Energy and Environmental Sciences, Paul Scherrer Institute, Forschungsstrasse 111, 5232, Villigen, Switzerland*
[b.] *Institute for Chemical and Bioengineering, ETH Zurich, Vladimir-Prelog-Weg 1, 8093, Zurich, Switzerland*
[c.] *CNR - Istituto Officina dei Materiali (IOM), Trieste, Laboratorio TASC, Strada Statale 14, km 163.5, 34149 Basovizza, Italy*
[d.] *Dipartimento di Fisica, Università degli Studi di Milano, Via Celoria 16, 20133 Milan, Italy*
[e.] *Centro Interdisciplinare Materiali e Interfacce Nanostrutturati (CIMAINA), Università degli Studi di Milano, Via Celoria 16, 20133 Milan, Italy*
† Present address: Interdisciplinary Nanoscience Center (iNANO), Aarhus University, 8000 Aarhus C, Denmark
‡ Present address: Scanning Probe Microscopy Laboratory, Department of Physics and Materials Science, University of Luxembourg, Luxembourg City L-1511, Luxembourg

Supporting Information

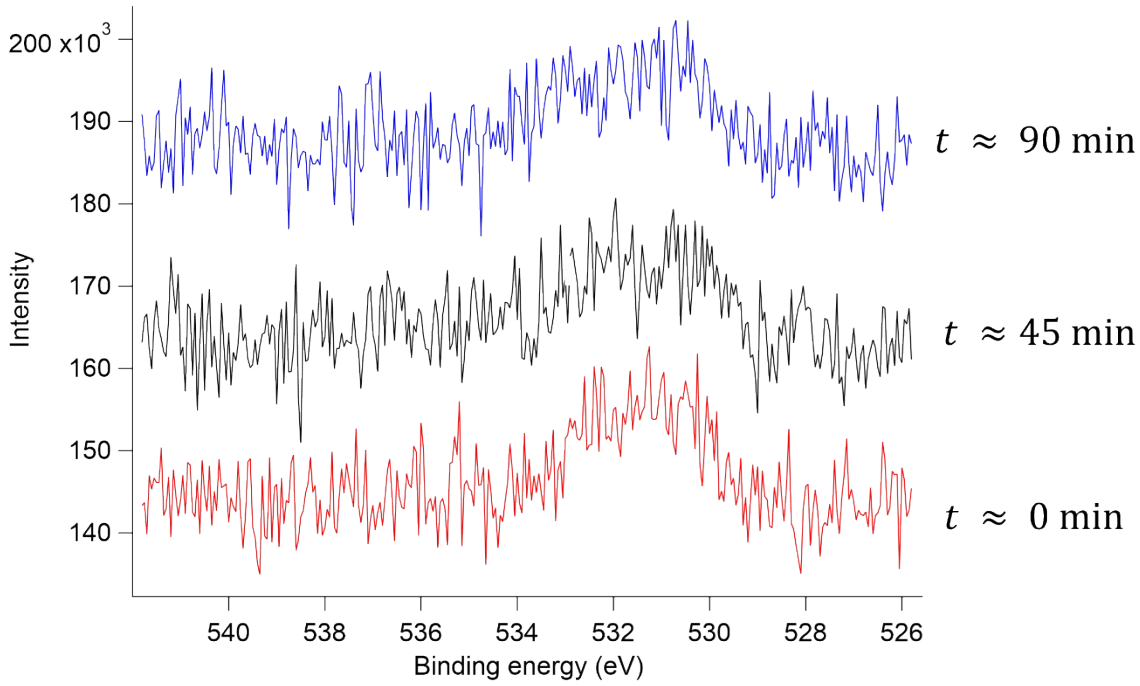

Figure S 1: O 1s spectra of the silver foil during exposure to 0.2 mbar H_2+CO_2 at 250°C, measured together with the carbon signals shown in Fig. 1a of the main manuscript. No increase in the O 1s signal can be detected over the course of 90 min of exposure. Measured at a photon energy of 684 eV.

S1: Carbon Coverage calculation

Ag 3d spectra were acquired at 520 eV at a pass energy of 50 eV (approx. 150 eV kinetic photoelectron energy E_{kin}), C 1s spectra were acquired at 437 eV at equal pass energy of 50 eV (approx. 150 eV E_{kin}).

The spectra were fitted using a Doniach-Sunjic approach with a convoluted Gaussian+Lorentzian curve.[1]

The total cross section for measurements with linearly polarized light and 90° between beam and analyzer was calculated using the following formula:

$$\sigma_t = \frac{\sigma}{4\pi}(1+\beta)$$

Here, σ_t denotes the total photoionization cross-section, σ is the cross-section for unpolarized light and β is the asymmetry parameter. Values were extracted from a publication by Yeh and Lindau[2] and are summarized in table S1. As molar volumes V_M the respective metallic molar volumes were used, for the carbon species the V_M of graphite was used. The inelastic mean free path of electrons with 150 eV kinetic energy was extracted from Tanuma et al.[3]

Table S 1: Values used to calculate the C-thickness on the Ag film.

	β	σ	σ_t	$V_{M,i}$ (cm3 mol-1)	λ_i (150eV)^i
C1s 437	2	0.38	0.09	5.82	5.2
Ag 3d 520	0.51	3.28	0.394	10.28	5.02
Cu2p 1086	1.14	0.774	0.132	7.09	5.6

The geometry of the growing metal-carbon system was assumed to be layered, as sketched in Fig. S2c.

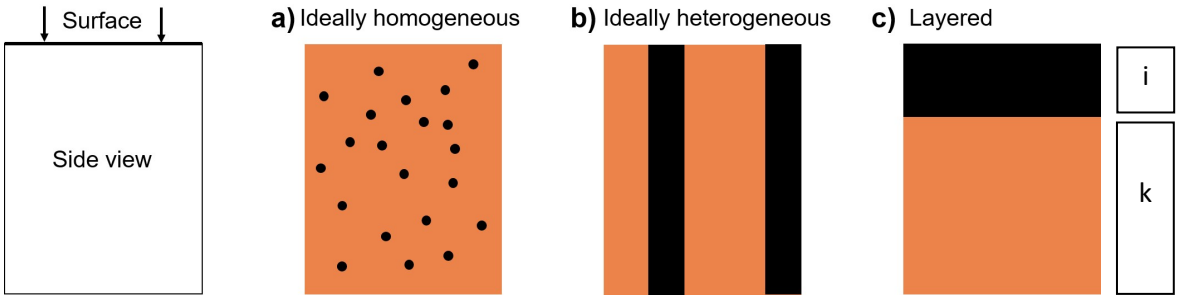

Figure S 2 Sketches of different simplified composite materials. The carbon impurity is assumed to deposit on the Ag metal in a layered way, as shown in c). Adapted from reference [4].

This leads to the following relation between the XPS signal intensity as a function of the thickness of the top material i:

$$\frac{I_i}{I_k} = \frac{I_{hv,i} V_{M,i} * \sigma_i * \lambda_i^*}{I_{hv,k} V_{M,k} * \sigma_k * \lambda_k^*}\left(e^{\frac{d}{\lambda_i^*}} - 1\right)$$

i = top layer, k = bulk

I = Intensity of the PE signal

$V_{M,i}$ = Molar Volume

σ_t= Photoemission total cross-section

λ_i^* = Angle-corrected IMFP of material I ($at\ PSI\ ISS\ beamline$: $\lambda_i^* = \lambda_i * \cos(\alpha = 30°) = \lambda_i * \frac{\sqrt{3}}{2}$)

d = thickness of top material i

$I_{hv,i}$ = Beam intensity (current measured at a photodiode)

Comment: The energy-dependent analyzer transmission function $\tau_i\ and\ \tau_k$ can be disregarded, as the kinetic energy of the photoelectrons is set to be equal, thus the transmission function of the analyzer is also equal

The equation is converted to isolate the thickness *d* on one side:

$$\ln\left[1 + \frac{I_i}{I_k} * \frac{I_{hv,k}}{I_{hv,i}} * \frac{V_{M,k} * \sigma_k * \lambda_k}{V_{M,i} * \sigma_i * \lambda_i}\right] * \lambda_i^* = d$$

The result is the value of *d* in Å, as the used IMFP is in Å. As an approximation, the layer of carbon species is assumed to be graphene (as also IMFP from graphite used), thus by dividing d by 3.35 Å/ML the thickness in ML is obtained.

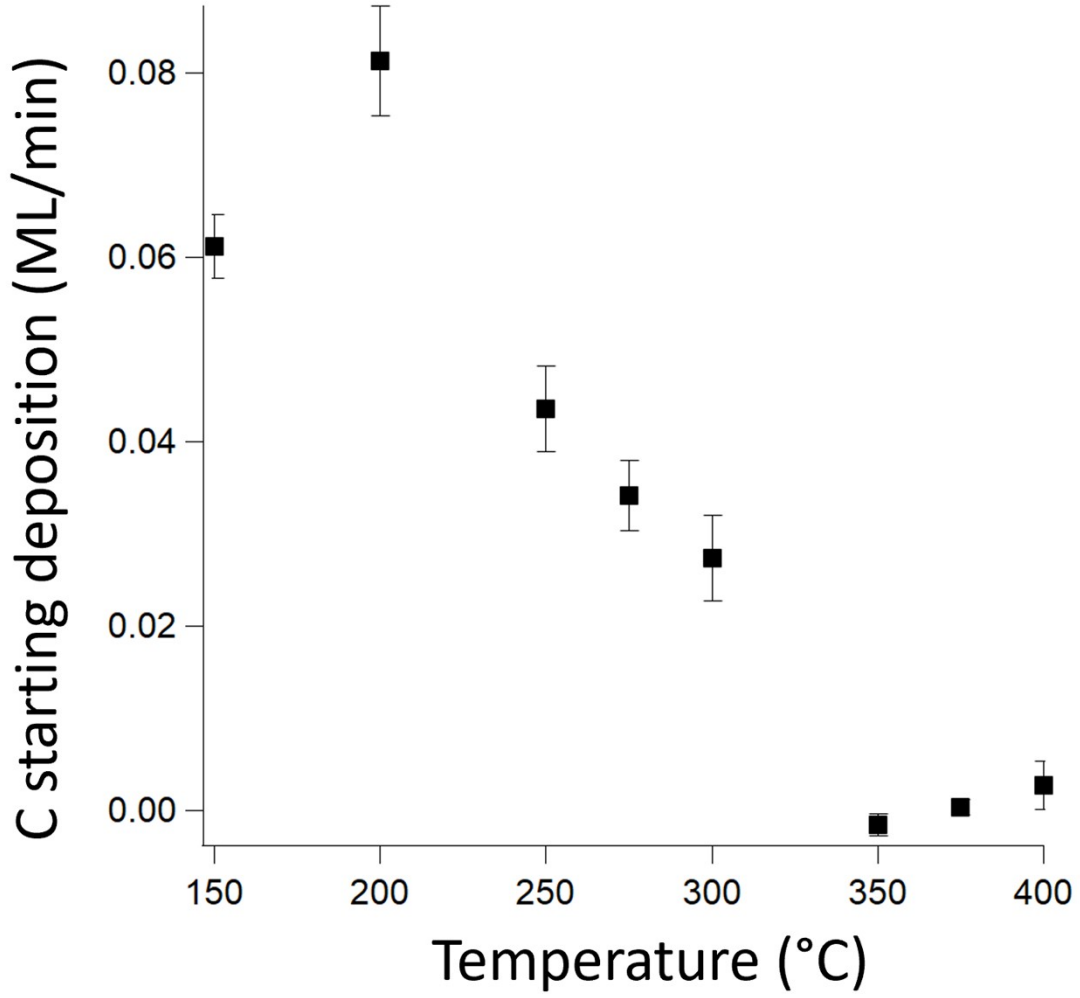

Figure S 3: Initial carbon deposition rate before the saturation effect sets in. The deposition rate shows a maximum at 200 °C and decreases with further increasing temperature, before dropping to 0 between 300 and 350°C.

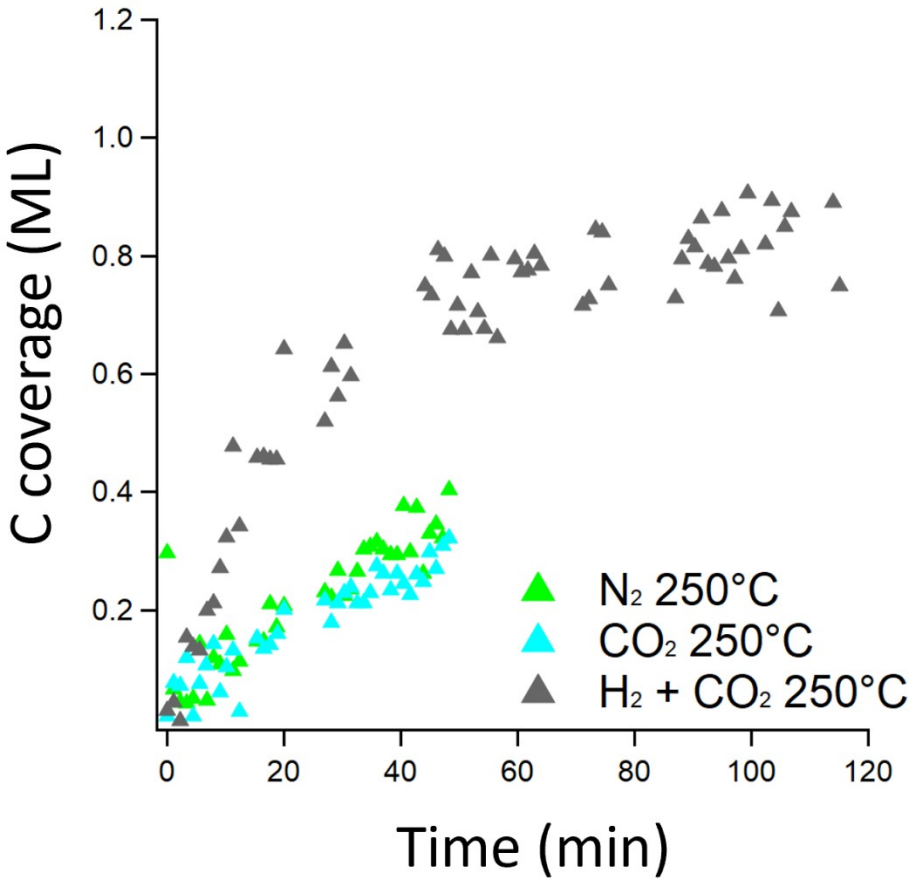

Figure S 4: Reference measurements with gases besides the reaction mixture on the silver foil.
Temporal evolution of the C 1s signal in N_2, CO_2 and in the reaction mixture (H_2 + CO_2) at 250 °C (total pressure always 0.2 mbar). The exposure to pure CO_2 and N_2 (with an impurity of CO_2, as can be seen in Fig. S5) indicates significantly slower carbon accumulation.

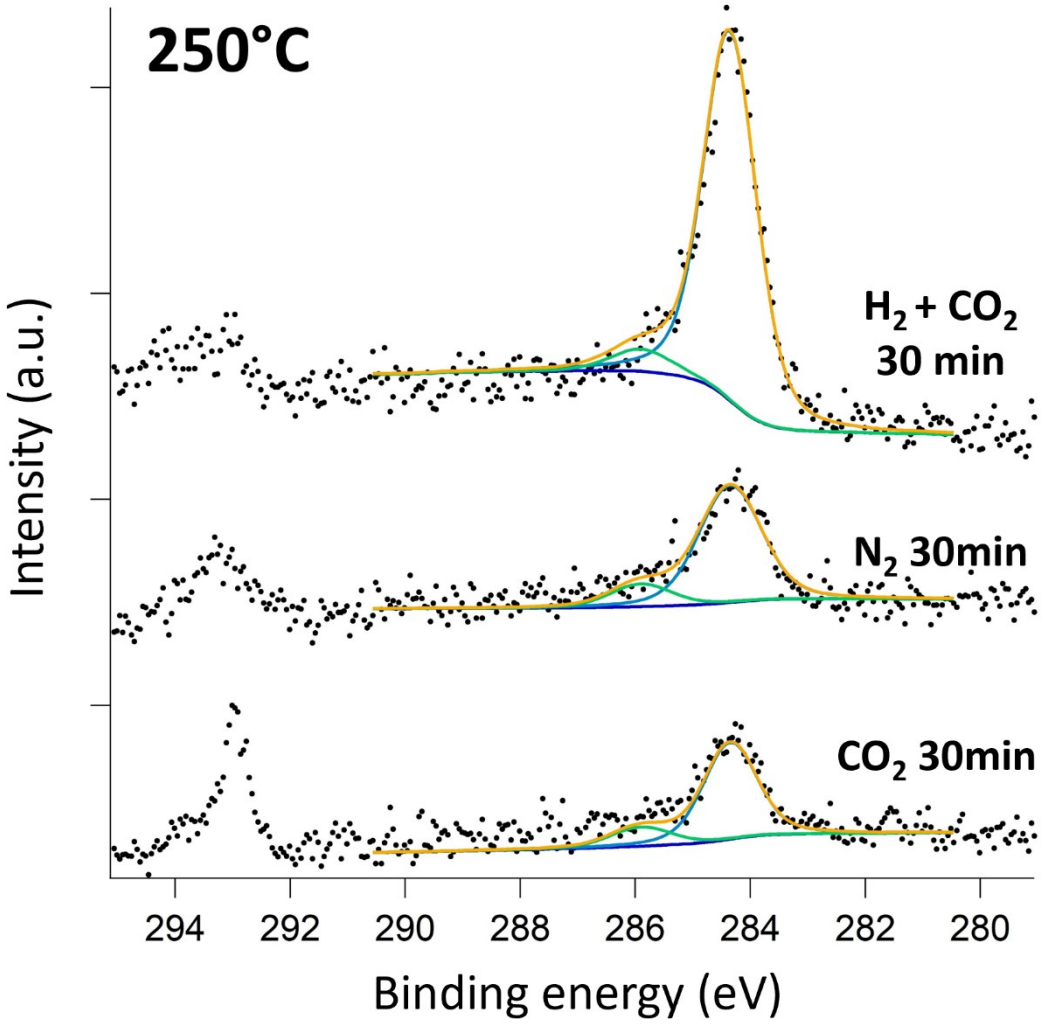

Figure S 5: Representative C 1s spectra of the reference measurements in H_2(+CO_2), CO_2 and N_2 (+CO_2) on silver at 250 °C (total pressure always 0.2 mbar). Spectra show the C 1s accumulation after approx. 30 min. The top spectrum shows a comparison to the C 1s spectrum obtained from exposure to reaction conditions (after approx. 30 min).

Table S 2: Measurement conditions for STM images shown in this work.

Figure	Bias voltage	Tunneling Current	Scan Speed	Image Size	Internal Reference
	mV	pA	nm/s	nm	
Main Text					
Fig. 2a)	-100	-800	200	30	VT231205_A1_0055
Fig. 2b)	-1000	-30	120	30	VT231205_A2_0026
Fig. 3a)	1800	10	20	20	VT231127_A2_0033
Fig. 3b)	1500	10	150	15	VT231211_A1_0095
Supporting Information					
Fig. S6a	-110	-1000	50	20	VT231205_A1_0064
Fig. S6b	-110	-1000	50	20	VT231205_A1_0063
Fig. S7a	-100	-800	200	50	VT231205_A1_0059
Fig. S7b	-110	-1000	50	50	VT231205_A1_0068
Fig. S8a	-500	-500	50	80	VT231205_A2_0107
Fig. S8b	-1000	-30	120	40	VT231205_A2_0023
Fig. S8c	-500	-500	50	20	VT231205_A2_0109
Fig. S11a	-100	-800	50	20	VT231127_A2_0075
Fig. S11b	1800	7	40	10	VT231127_A2_0045
Fig. S11c	-800	-20	50	50	VT231127_A2_0079
Fig. S12a	1500	10	150	15	VT231211_A1_0095
Fig. S12b	1500	10	50	10	VT231211_A1_0064
Fig. S13a	1000	150	150	15	VT231211_A1_0111
Fig. S13b	1000	150	150	8	VT231211_A1_0114
Fig. S14a	1500	10	50	10	VT231211_A1_0065
Fig. S14b	1500	10	150	10	VT231211_A1_0069
Fig. S14c	1500	300	150	20	VT231211_A1_0076

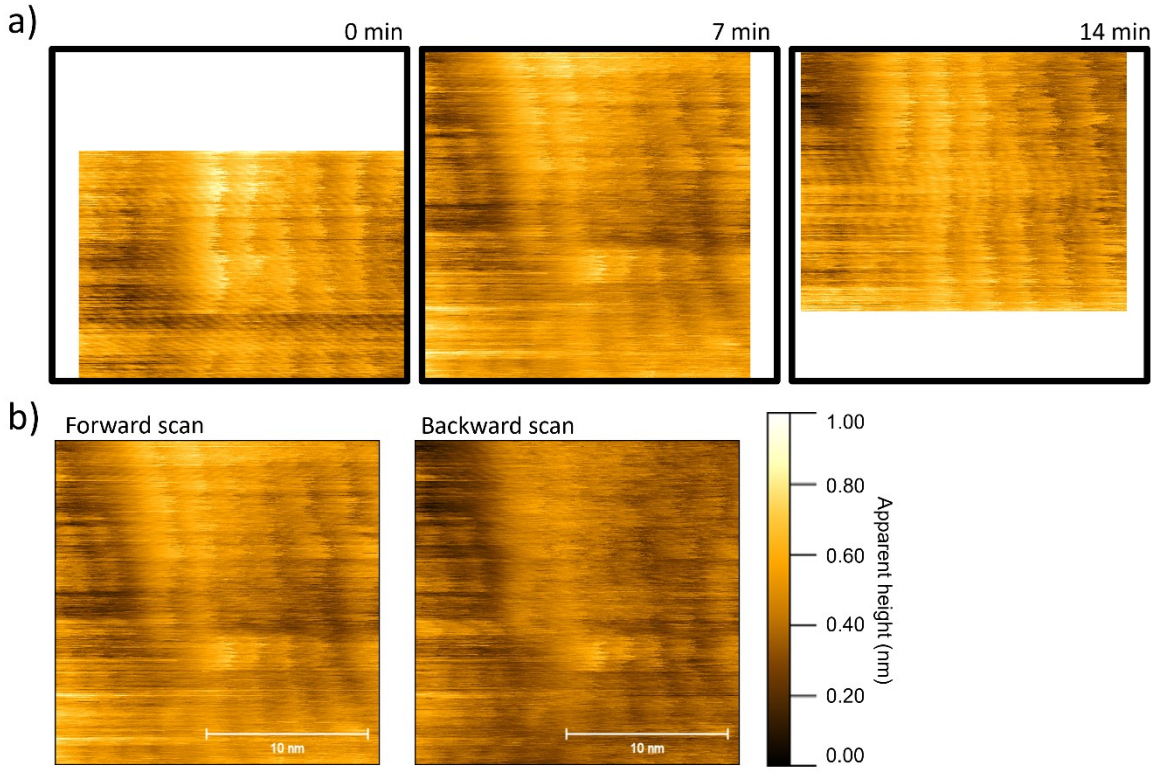

Figure S 6: High fluctuations of Ag steps in the clean state. STM images of the clean Ag film heated to 375°C.
a) Same area over the course of several images obtained with approx. 7 min delay.
b) Comparison of the forward and backward scan on the same area.

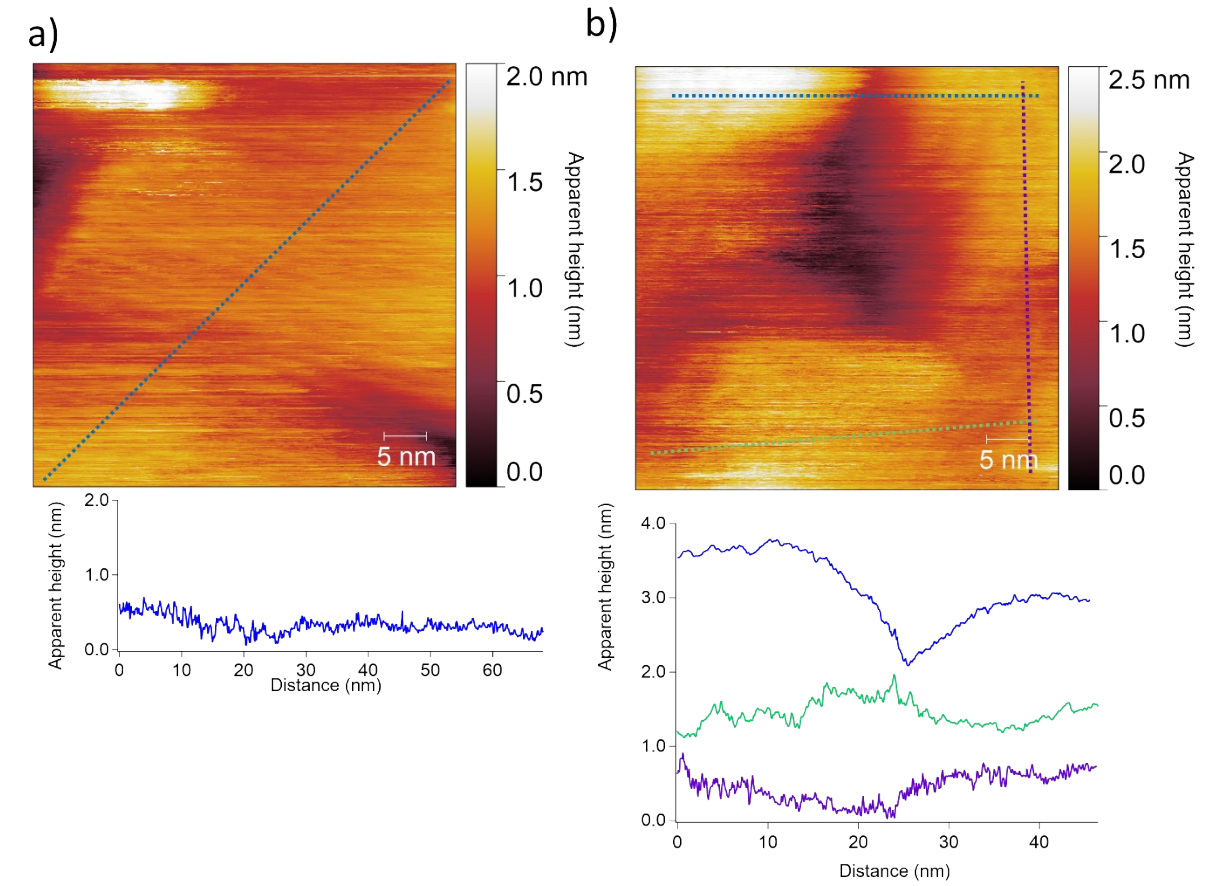

Figure S 7: Further images of the clean silver surface treated at high-temperature conditions. Line scans are shown below each respective image.

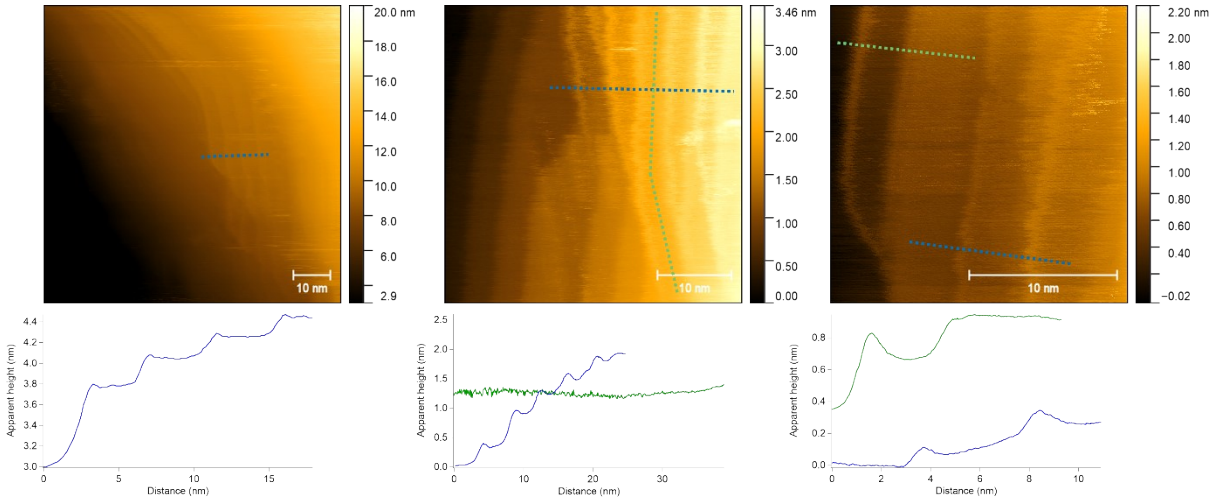

Figure S 8: Further images of the contaminated silver surface treated at 200°C in 1 mbar H_2+CO_2. Line scans are shown below each respective image.

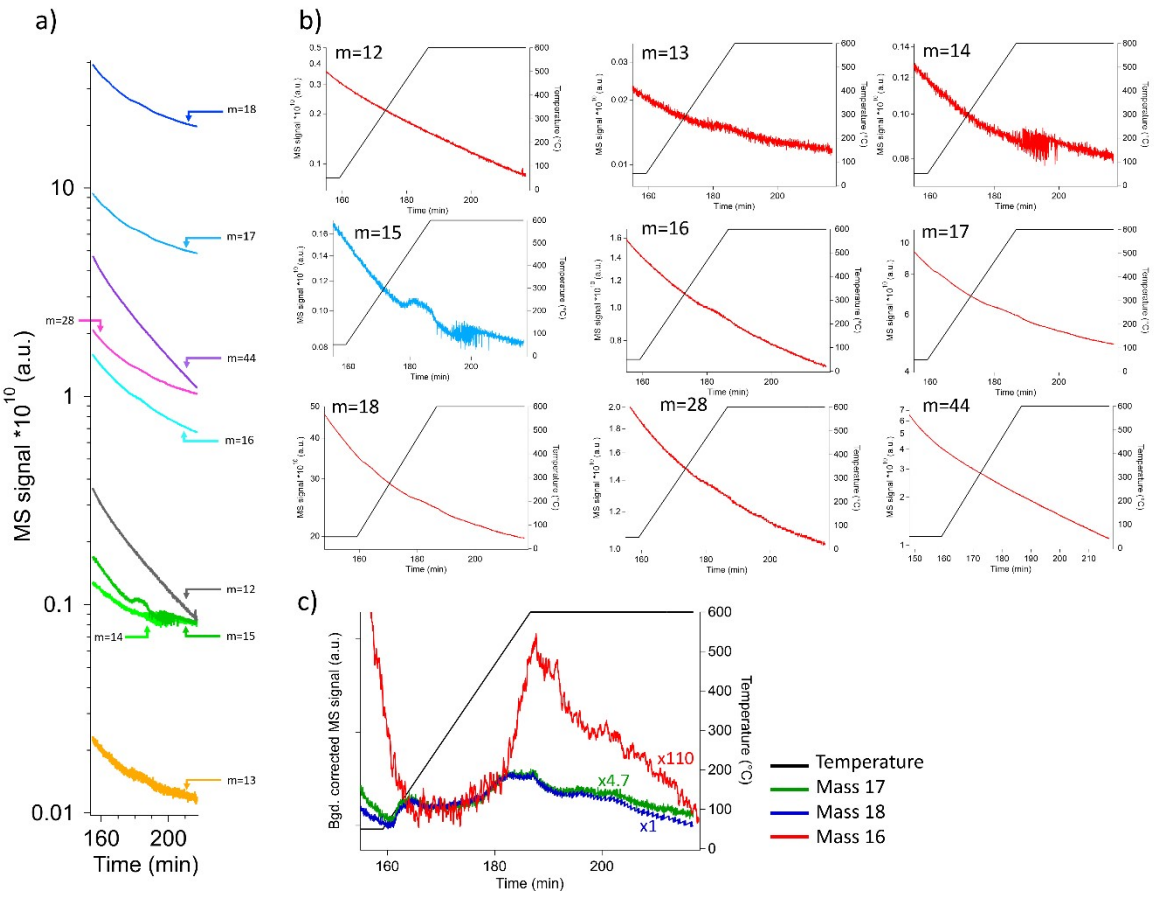

Figure S 9: H_2-TPR traces of several masses recorded by MS. No signal can be resolved for any mass except m=15 a.m.u., indicating methane, and masses related to water traces (m=16, 17, 18). Further mass fragments of methane, m=14, 13 and 12 a.m.u. have a signal intensity of <20% with respect to the signal of m=15.[5] Those signals cannot be resolved.

a) All spectra in one single logarithmic plot.

b Spectra plotted individuallz on a logarithmic scale.

c) The signals of water, m=16, 17 and 18 a.m.u. are normalized by the fragmentation probability in an MS-spectrum of water (electron ionization, NIST-Standard reference database).[5] Signal m=16 (red) shows a higher normalized signal compared to the other mass fragments in water, reassuring the signal superposition of water and methane for mass 16.

AFM Statistics

The topographic image in Fig. S10a has been acquired in Tapping Mode in air using a Bioscope Catalyst AFM from Bruker. The particle size (height) distribution has been determined using custom Matlab routines.

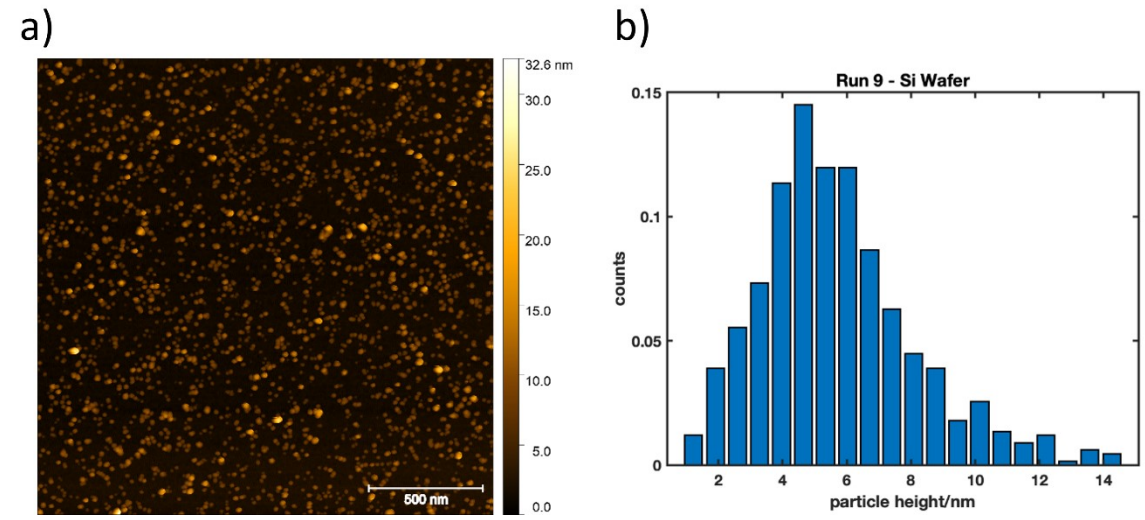

Figure S 10: AFM measurements on zinc oxide nanoparticles deposited on a silicon wafer for statistical analysis.
a) Atomic force microscopy (AFM) image of the sample.
b) Statistical analysis of the cluster size detected in a). The size analysis leads to a mean particle size of 5.4±2.6 nm.

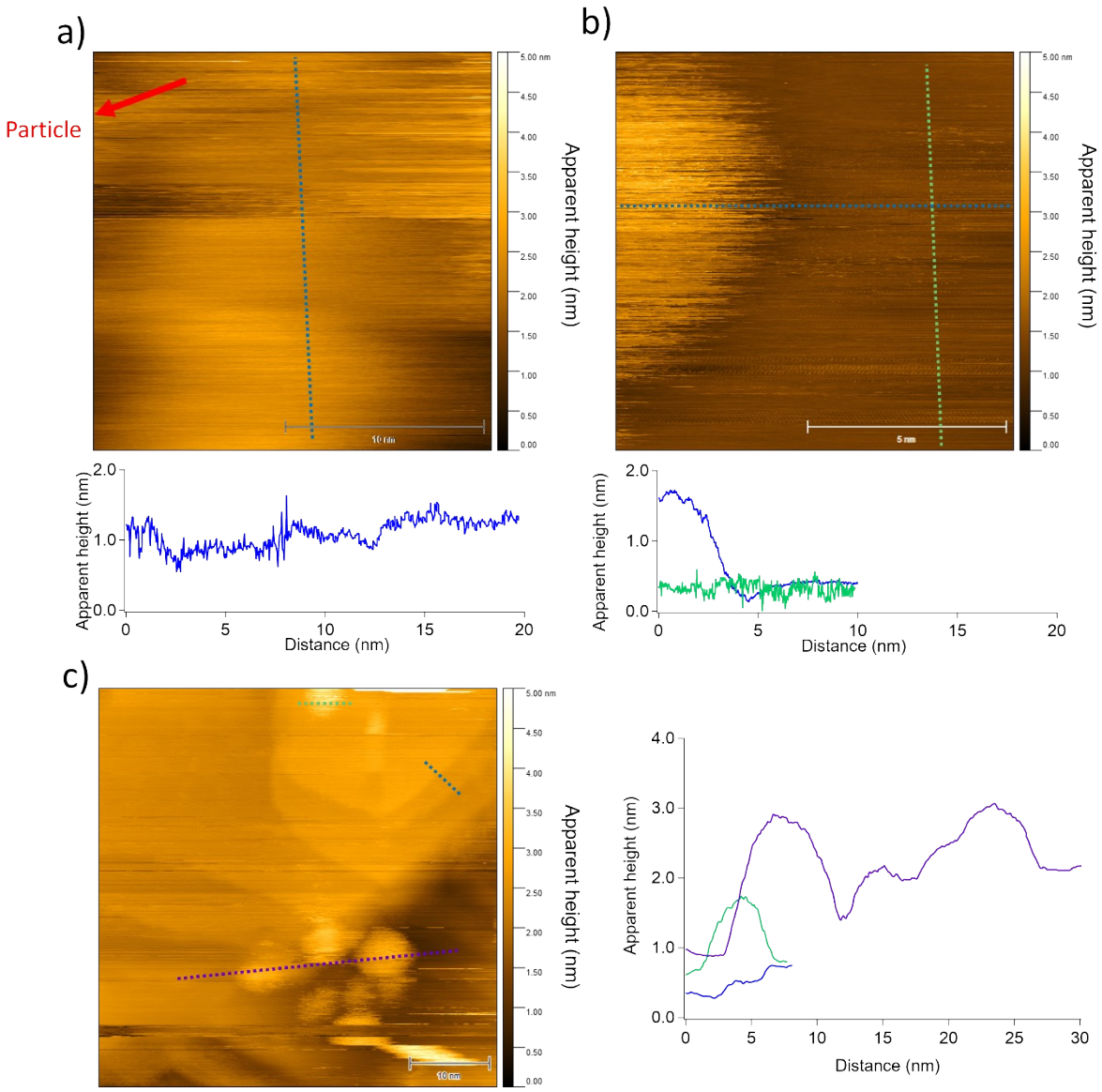

Figure S 11: Further images of the clean Ag+ZnO surface treated at high-temperature conditions.

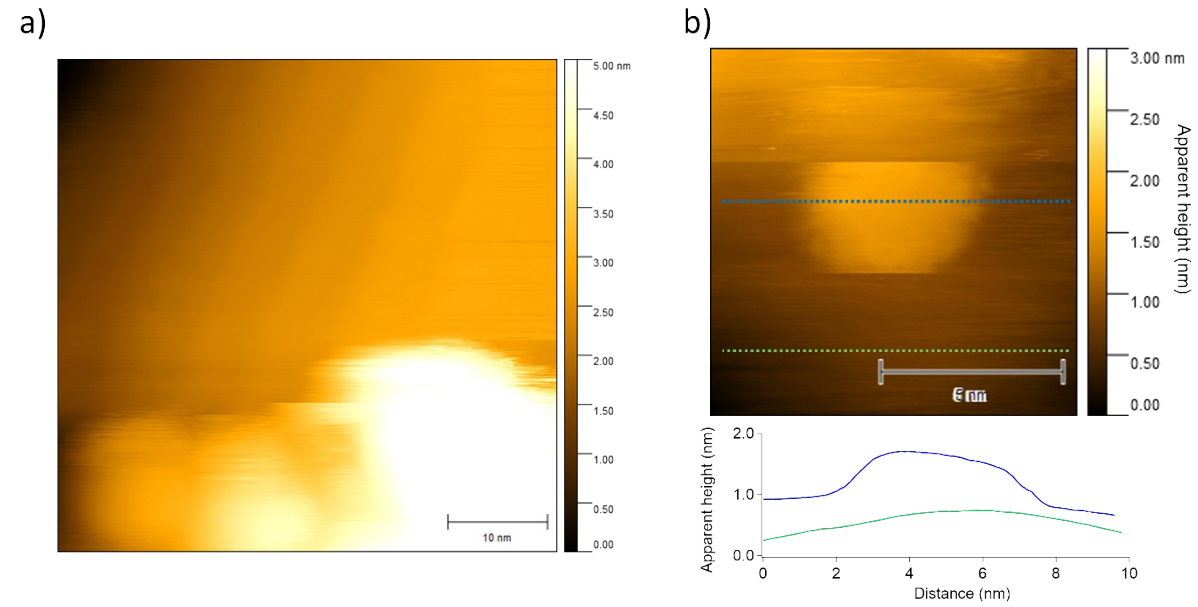

Figure S 12: Further images of the contaminated Ag+ZnO surface treated at 200°C in 1 mbar H_2+CO_2. Line scans are shown below each respective image. a) shows the complete image shown in the main manuscript.

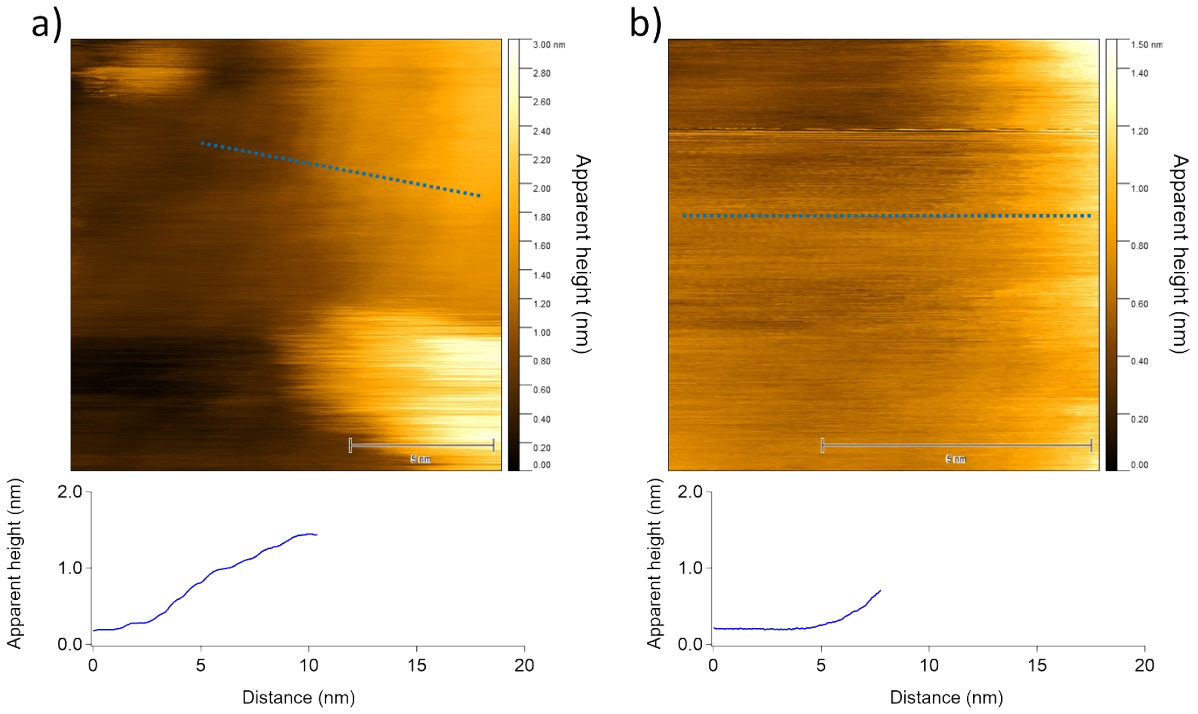

Figure S 13: Further images of the contaminated Ag+ZnO surface treated at 200°C in 1 mbar H_2+CO_2. Line scans are shown below each respective image. b) shows a magnified region of a).

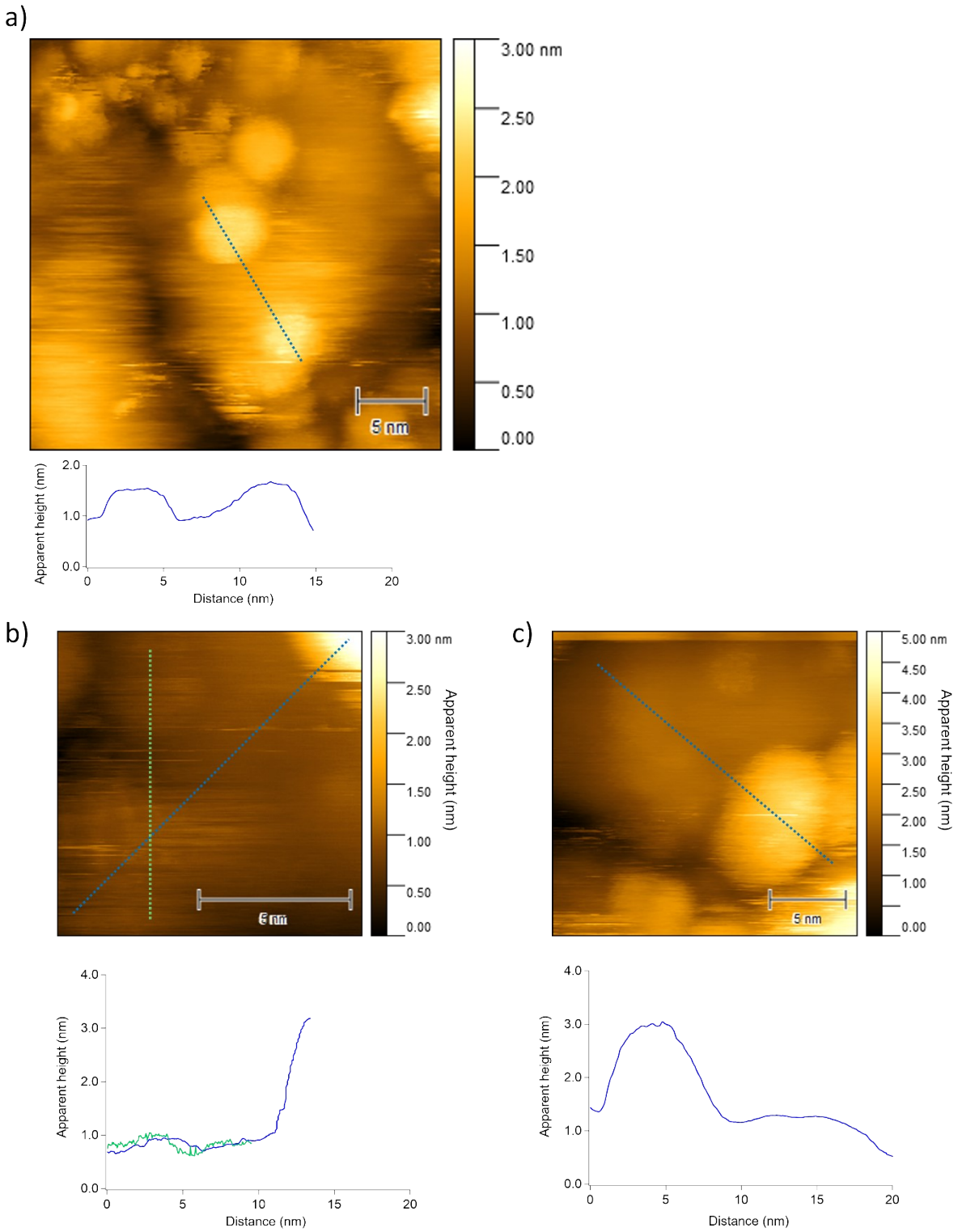

Figure S 14: Further images of the contaminated Ag+ZnO surface treated at 200°C in 1 mbar H_2+CO_2. Line scans are shown below each respective image. b) shows a magnified region of a).

LEED analysis

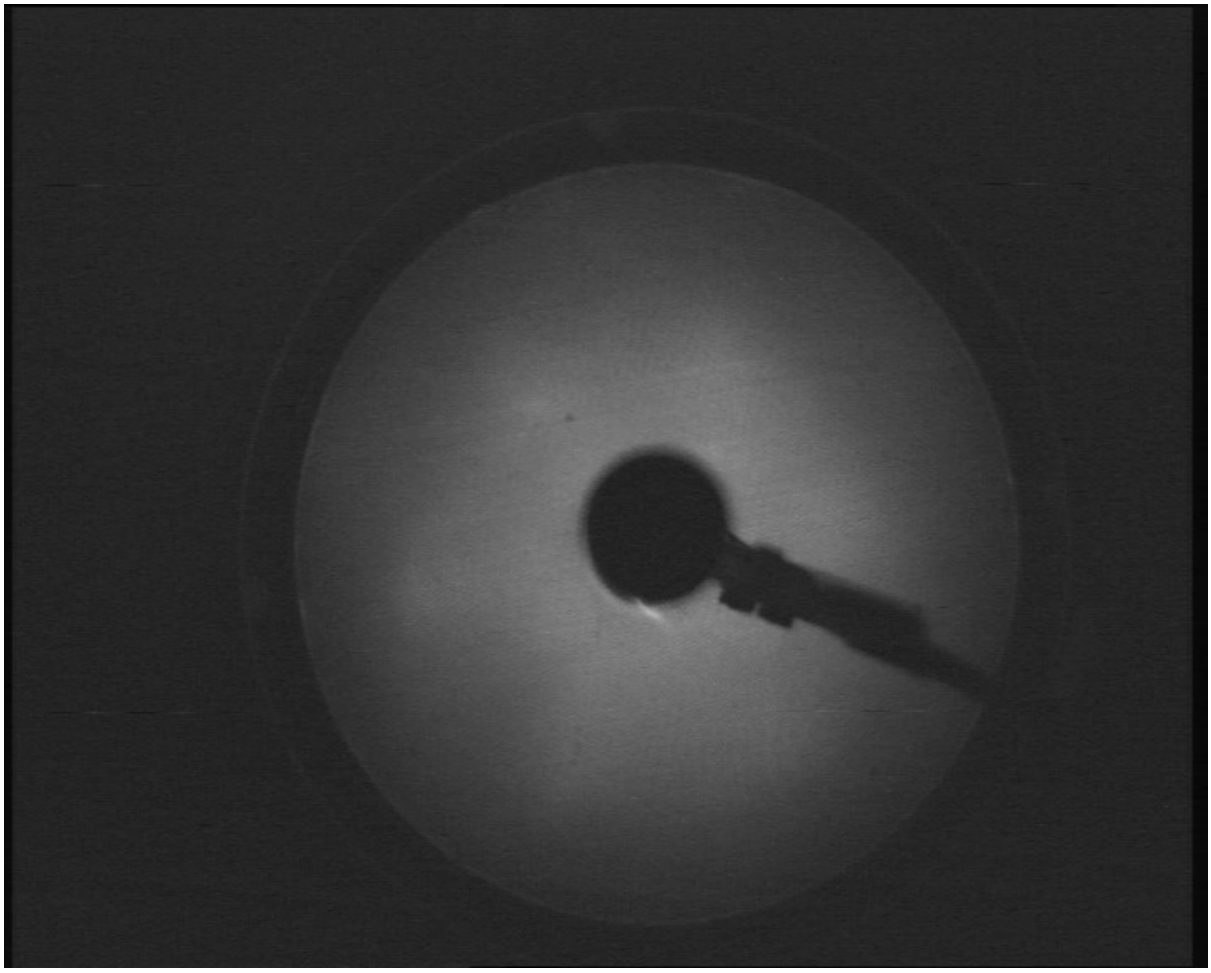

Figure S 15: Low Energy Electron Diffraction (LEED) image of the 200 nm Ag/5 nm Cr film on Mica substrate, sputtered by high-energy Ar-ions and annealed in vacuum to 450 °C for several cycles. Electron energy: 132 eV.

XPS Silver signal

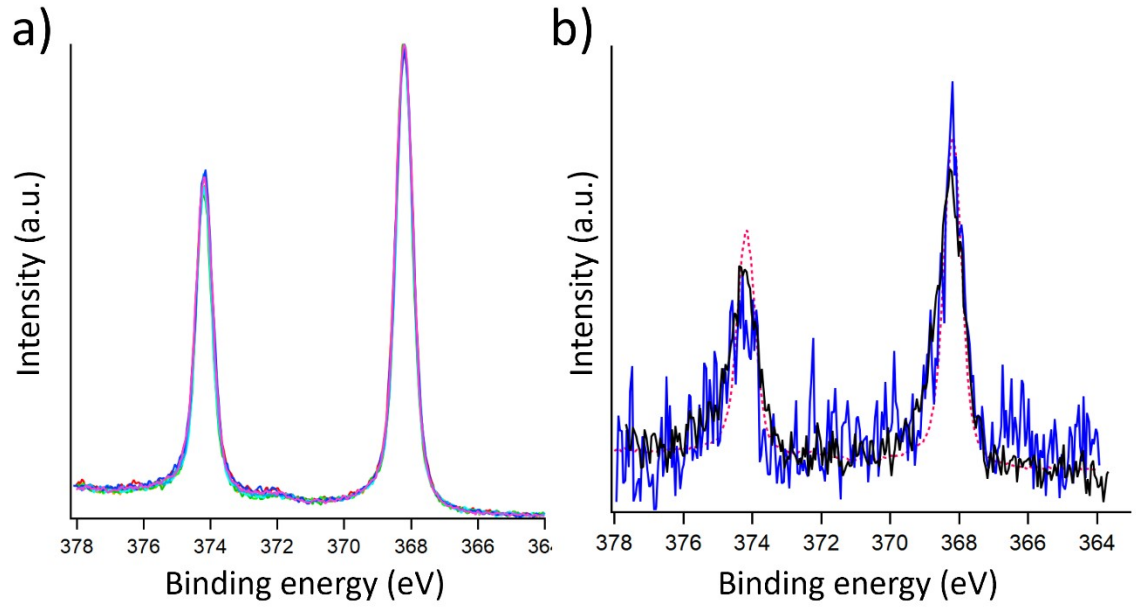

Figure S 16: Ag 3d signal of all samples used for energy calibration and contaminant quantification.
a) Normalized and superimposed spectra of all pure Ag films in clean and contaminated state at 200°C, 250°C, 300°C, 350°C. All Spectra measured at 520 eV.
b) Spectra of Ag 3d for the Ag/ZnO material measured at 520 eV (blue) and 684 eV (black) photon energy. The dotted spectrum shows a reference of pure silver. Partial charging was observed in several cases for the Ag/ZnO high surface area material.

XRD

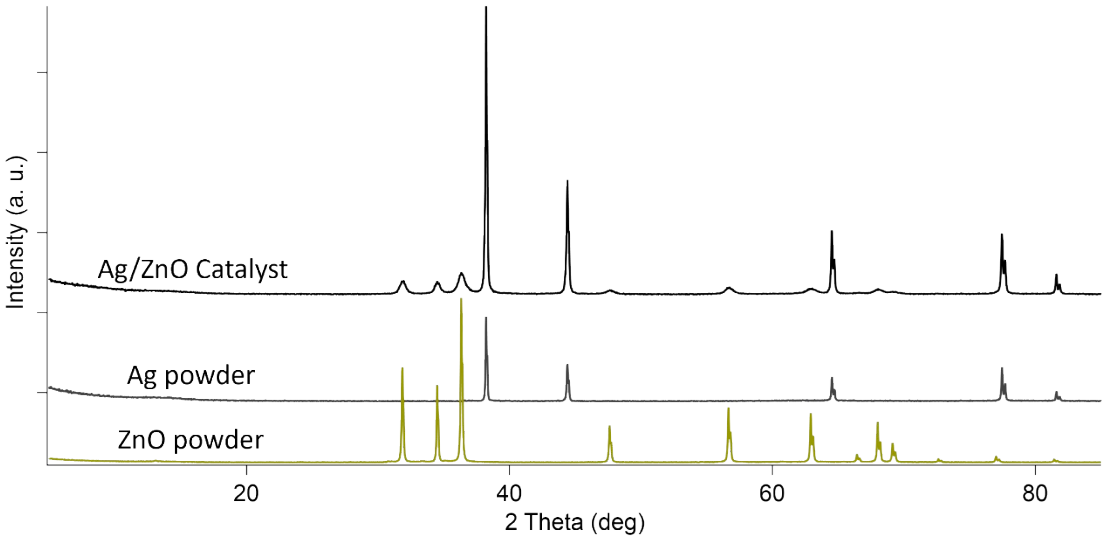

Figure S 17: XRD spectra of the Ag/ZnO material and reference spectra obtained for Ag and ZnO. This material is also used and thoroughly described elsewhere.[6]

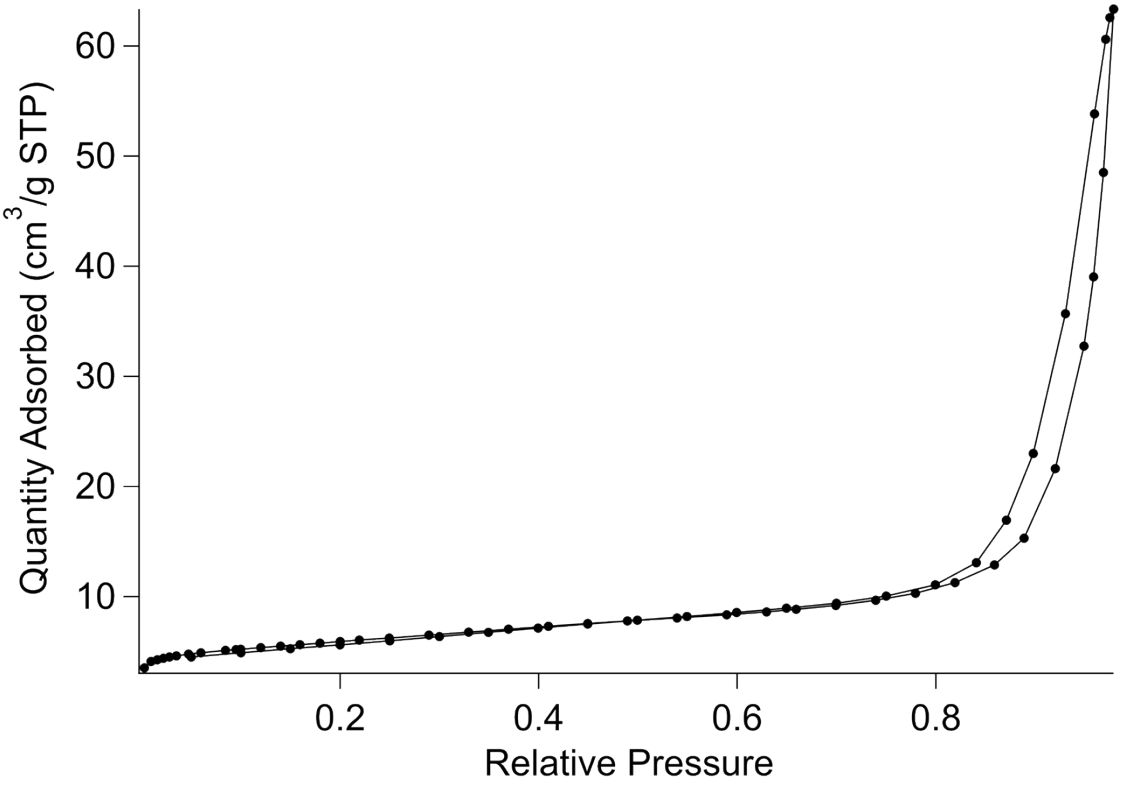

Figure S 18: Nitrogen adsorption relation of the synthesized Ag/ZnO material.

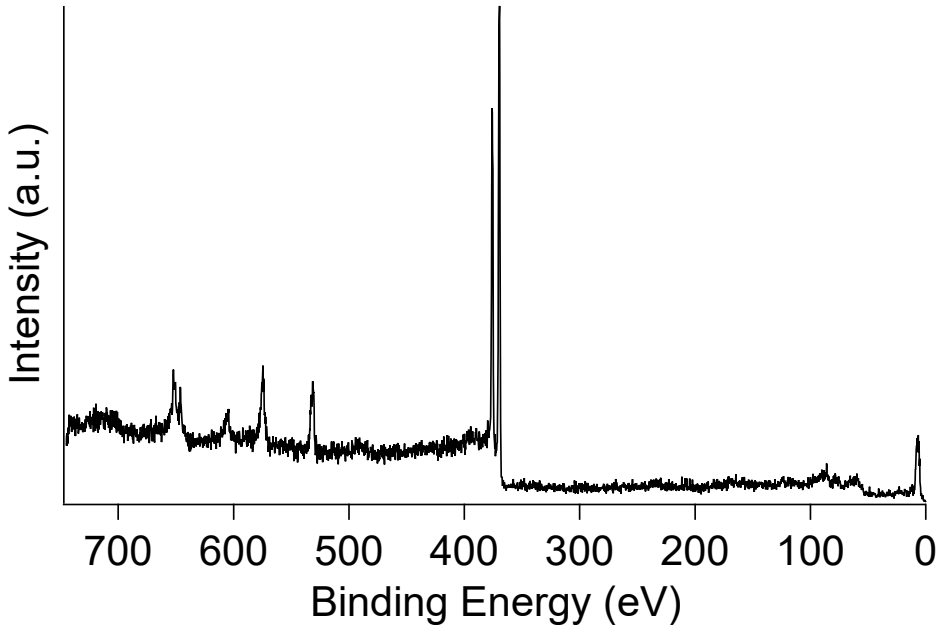

Figure S 19: XPS survey spectrum of the silver powder used for H_2-TPR after heating to 400°C in vacuum, measured at a photon energy of 1000 eV. The C 1s signal cannot be detected in the survey spectrum, while the O 1s signal is present.

References

1 Doniach, S. & Sunjic, M. Many-electron singularity in X-ray photoemission and X-ray line spectra from metals. *Journal of Physics C: Solid State Physics* **3**, 285 (1970).

2 Yeh, J. J. & Lindau, I. Atomic Subshell Photoionization Cross-Sections and Asymmetry Parameters - 1 Less-Than-or-Equal-to Z Less-Than-or-Equal-to 103. *Atom Data Nucl Data* **32**, 1-155 (1985). https://doi.org/Doi 10.1016/0092-640x(85)90016-6

3 Tanuma, S., Powell, C. J. & Penn, D. R. Calculations of electron inelastic mean free paths. IX. Data for 41 elemental solids over the 50 eV to 30 keV range. *Surf. Interface Anal.* **43**, 689-713 (2011). https://doi.org/10.1002/sia.3522

4 Leidinger, P. *Synthesis of supported and freestanding graphene: fundamental understanding of the reaction thermodynamics and kinetics on Cu* PhD thesis, Technical University of Munich (TUM), (2022).

5 *NIST Standard Reference Database 71*, 2019).

6 Leidinger, P. M. *et al.* Influence of alumina on the performance of Ag/ZnO based catalysts for carbon dioxide hydrogenation. *Journal of Catalysis* **440** (2024). https://doi.org/10.1016/j.jcat.2024.115837